

Femtosecond relaxation of photoexcited states in nanosized semiconductor particles of iron oxides

V. A. Nadtochenko,^{a*} N. N. Denisov,^a V. Yu. Gak,^a F. E. Gostev,^b A. A. Titov,^b O. M. Sarkisov,^b and V. V. Nikandrov^c

^a*Institute of Problems of Chemical Physics, Russian Academy of Sciences,
142432 Chernogolovka, Moscow Region, Russian Federation.
Fax: +7 (096) 515 3588. E-mail: nadto@icp.ac.ru*

^b*N. N. Semenov Institute of Chemical Physics, Russian Academy of Sciences,
4 ul. Kosygina, 119991 Moscow, Russian Federation.
Fax: +7 (095) 938 2156. E-mail: udod@femto.chph.ras.ru*

^c*A. N. Bach Institute of Biochemistry, Russian Academy of Sciences,
4 Leninsky prosp., 119991 Moscow, Russian Federation.
Fax: +7 (095) 954 2732. E-mail: nikandr@mx.inbi.ras.ru*

Relaxation of photoexcited states in nanosized semiconductor particles of iron oxides was studied by femtosecond laser photolysis techniques: (1) in an aqueous colloidal solution of α -Fe₂O₃; (2) in Fe₂O₃ particles in the Nafion[®] cation-exchange polymeric membrane; (3) in an aqueous colloid of γ -Fe₂O₃; and (4) in nanocrystals of ferrihydrite 5Fe₂O₃·9H₂O, which are contained in the protein shell of ferritine. The photoinduced excited states relax at the femtosecond and picosecond time scale. The spectra of photoinduced absorption of photoexcited states and the relaxation dynamics in the studied iron oxides weakly depend on the structure and surface environment of a nanoparticle.

Key words: femtosecond spectroscopy, iron oxides, femtosecond dynamics, ferritine, photocatalysis.

Nanosized particles of iron oxide/hydroxides are used as pigments,¹ semiconductor photocatalysts, and magnetic materials.^{1–13} Colloidal solutions of iron oxides play an important role in biological and biogeochemical systems.^{14–17}

The aim of this work is to study the dynamics of photoexcited states for different forms of iron oxide: nanosized particles of α -Fe₂O₃ in the form of an aqueous colloidal solution; nanosized particles of a mixture of two oxide forms α - and γ -Fe₂O₃ in the Nafion[®] cation-exchange polymeric matrix; nanosized particles of an aqueous colloidal solution of γ -Fe₂O₃; and nanosized crystals of ferrihydrite hydroxide 5Fe₂O₃·9H₂O, which are contained in the protein shell of ferritine, *viz.*, protein playing a fundamental role in iron metabolism in living organisms.^{16,17} Ferritine exhibits photochemical activity, which is associated with the presence of ferrihydrite.^{18,19} The listed forms of Fe₂O₃ differ in structure of the crystalline lattice, magnetic properties, and surface environment. The authors²⁰ recently reported the dynamics of photoexcited states in colloids of α - and γ -Fe₂O₃ upon excitation with a light pulse with a wavelength of 390 nm and probing with a light of 720 nm. In this work, both the data on the absorption spectra of photoexcited states in semiconductor particles of iron oxide and more complete data on the

kinetics of their relaxation are presented for the first time. Iron oxides are presented in more various forms than those in the previous work.²⁰ The data on photoexcited states of nanoparticles of iron oxides will allow more complete understanding of the nature of their photocatalytic and photoelectrochemical properties.

Experimental

Preparation of samples. Colloidal solutions. Colloidal solutions of α -Fe₂O₃ were prepared according to a previously published procedure.²³ The initial solution of FeCl₃·6H₂O (0.050 mol L⁻¹) was added dropwise to a 20-fold volume of boiling distilled water. The solution that formed had an intense red color without opalescence. According to the published data,²³ the particle size ranged from 2 to 25 nm.

Solutions of γ -Fe₂O₃ were prepared by the dropwise addition of a solution of FeCl₃·6H₂O and FeCl₂·4H₂O (Fluka) to a 1 M solution of NaOH followed by acidification to pH 3.5 with hydrochloric acid. At the final stage of preparation, air was bubbled through the solution, and the latter was centrifuged. The average particle size was 10 nm.²⁰

Polymeric membrane Nafion[®]. The Nafion[®] film (Aldrich) was purified by heating in a 10% solution of H₂O₂ with an additive of 10% sulfuric acid.

Nanosized Fe₂O₃ particles in Nafion[®] were obtained as follows. The film was first stored in a 1 M solution of FeCl₃·6H₂O

for 3 h, washed with distilled water, and then placed in a 0.5 M solution of NaOH for 1 h. The formation of Fe_2O_3 was monitored by UV-Vis, IR, and Mössbauer spectroscopies and measuring magnetic susceptibility. The main phase is $\alpha\text{-Fe}_2\text{O}_3$ with an admixture of the ferromagnetic phase, which was assigned to $\gamma\text{-Fe}_2\text{O}_3$. We failed to determine quantitatively the ratio of two phases.

Ferritine. Commercial ferritine isolated from horse spleen (Sigma, 108 mg mL^{-1} , 800 Fe atoms per protein molecule in a 0.15 M solution of NaCl) and ferritine (Fluka, 108 mg mL^{-1} , 2000 Fe atoms per protein molecule in H_2O) were used. Before measurements, samples were diluted with distilled water. Apoferritine (iron-free ferritine) (Sigma) was diluted to the concentration corresponding to the protein concentration in the experimental ferritine samples.

Femtosecond photolysis. The dynamics of excitons and electron-hole pairs in nanosized iron oxide particles was studied using a femtosecond laser kinetic spectrometer.²⁴ Pulses with a duration of 60 fs and an energy of 0.1 nJ at a wavelength of 610–620 nm were generated by a CPM dye laser with a repetition frequency of 10^8 Hz. The sequence of pulses with a duration of 50 fs, an energy of 300 μJ , and a repetition frequency of 25 Hz was achieved at the outlet after a two-cascade laser amplifier pumped by radiation pulses of the second harmonic of an Nd:YAG laser (energy 40 mJ, duration 8 ns, $\lambda = 532$ nm, pulse recurrence frequency 25 Hz) and a compressor.

Measurements were performed by the pump probe technique: the second harmonic pulse (308 nm) was used for excitation, and the energy was varied from 3 to 20 μJ . The probe pulse was a pulse of supercontinuum, which was generated by focusing of a femtosecond pulse in a quartz cell with a thickness of 4 mm filled with a $\text{D}_2\text{O} : \text{H}_2\text{O}$ (1 : 1) mixture. The procedure of measuring spectra and the absorption kinetics using white supercontinuum has been described earlier.²⁵ The value of absorption $\Delta A_\lambda(t) = A_\lambda(t) - A_\lambda(0)$ was measured, where $A_\lambda(t)$ is the absorption of the sample in the moment t after a laser pulse, and $A_\lambda(0)$ is the absorption before excitation.

Colloidal solutions of iron oxides were pumped through a cell 1 mm thick. The sample was immobile in experiments with the Nafion® films. This did not change the findings because the results of measurements were completely reproduced at repeated scans of the immovable sample. The densities of pump and probe power were selected in such a way that the maximum signal-to-noise ratio was achieved and undesirable signals from nonlinear optical processes were avoided. Experiments were conducted in air at 293 K.

Results and Discussion

The studied forms of iron oxide ($\alpha\text{-Fe}_2\text{O}_3$, $\gamma\text{-Fe}_2\text{O}_3$, Fe_2O_3 in Nafion® and in ferrihydrite in the protein shell of ferritine) exhibit a broad-band (from 400 to 1000 nm) short-lived photoinduced absorption, which is characterized by a considerable resemblance of both the curve of absorption decay and transient absorption spectra for all four forms of oxides. The most substantial experimental facts concerning photoinduced absorption and its relaxation can be summarized as follows.

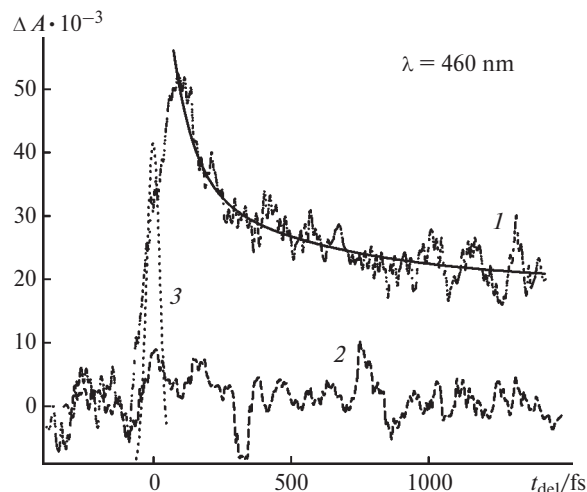


Fig. 1. Photoinduced absorption of ferrihydrite $\text{Fe}_2\text{O}_3 \cdot 9\text{H}_2\text{O}$ formed in the protein shell of ferritine: 1, ferrihydrite $\text{Fe}_2\text{O}_3 \cdot 9\text{H}_2\text{O}$ in ferritine (solid line is the result of approximation of the decay by the function $A_1 \exp(-t/\tau_1) + A_2 \exp(-t/\tau_2)$); 2, apoferritine (ferritine without ferrihydrite); and 3, time point spread function in experiment.

1. Absorption in all four samples is caused by iron oxide particles only. This can be exemplified by the photoinduced absorption curve for ferritine with iron hydroxide and the curve observed for the excitation of apoferritine, *viz.*, protein shell of ferritine containing no ferrihydrite (Fig. 1). As can be seen, under the experimental conditions, we can neglect the absorption signal related to the excitation of tryptophan and tyrosine amino acids in the protein, and in the case of aqueous colloids and Nafion®, the signals due to the interaction of femtosecond light pulses with water and the film can also be neglected.

2. The photoinduced absorption decay in $\alpha\text{-Fe}_2\text{O}_3$, $\gamma\text{-Fe}_2\text{O}_3$, Fe_2O_3 in Nafion®, and ferrihydrite is determined by a polyexponential time law. This is confirmed by the kinetic curve of absorption decay for ferrihydrite (see Fig. 1) and an analogous curve for a colloidal solution of $\alpha\text{-Fe}_2\text{O}_3$ (Fig. 2). These curves are typical of all studied samples: the leading edge of the absorption curve is determined by the pulse duration. This behavior of absorption curve is characteristic of all samples in the whole spectral range studied (400–1000 nm). The time law of absorption decay is the same for different wavelengths of the same sample within an experimental error. The decay curve in time windows of 0–6 ps was approximated by the equation $A_1 \exp(-t/\tau_1) + A_2 \exp(-t/\tau_2)$. The parameters A_1 , A_2 and τ_1 , τ_2 obtained from the experimental curve are presented in Table 1. For the samples of a colloidal solution of $\alpha\text{-Fe}_2\text{O}_3$, we achieved a higher signal-to-noise ratio and quantitatively expand the decay curve in the time window to 50 ps by the three-exponential law

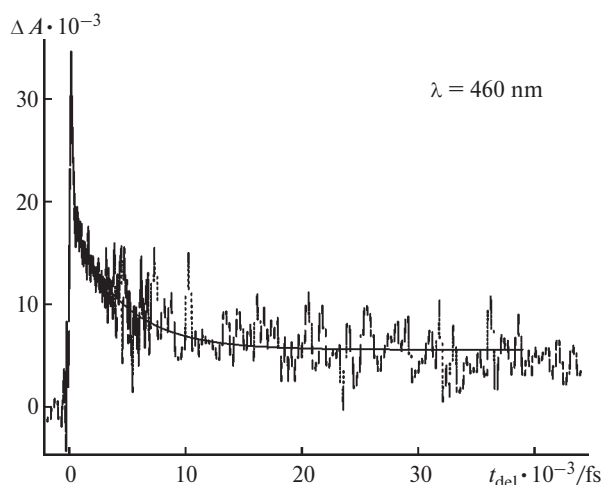


Fig. 2. Photoinduced absorption of α -Fe₂O₃ (solid line is the result of approximation of the decay by the function $A_1\exp(-t/\tau_1) + A_2\exp(-t/\tau_2) + A_3\exp(-t/\tau_3)$).

$A_1\exp(-t/\tau_1) + A_2\exp(-t/\tau_2) + A_3\exp(-t/\tau_3)$. The inverse time (τ_3^{-1}) for the slow component is $(2.6 \pm 0.6) \cdot 10^{-5} \text{ fs}^{-1}$.

3. No change in the time law of the photoinduced absorption decay was found with changing the density of the excitation power of samples, *i.e.*, the initial concentration of excited states has no effect on the profile of the curve.

4. The transient absorption spectra presented for all studied forms of iron oxides in Fig. 3 are qualitatively similar: these are broad-band spectra with rather intense absorption in the short-wave spectral region and a weaker band in the long-wave region.

The characteristic relaxation times for two fastest components of the curve of absorption decay in α -Fe₂O₃ and γ -Fe₂O₃ upon excitation (310 nm, 3.77 eV, this work) are close to the relaxation times of the components in α -Fe₂O₃ and γ -Fe₂O₃ upon excitation with $\lambda = 390 \text{ nm}$ (3 eV, see Ref. 20). This fact indicates that the excess energy of photogenerated carriers relaxes rapidly within the resolution time of the laser (75 fs).

Based on the published data on the spectral properties of the iron oxides^{21,22} and absorption spectra of electrons in the valence band injected by pulse radiolysis, we can draw certain conclusions about the nature of carriers, which cause femtosecond photoinduced absorption. The absorption of the iron oxide in the visible range of 2.2 eV (565 nm) is due to the d–d transitions of iron, whereas the resolved transition from the 2p orbitals of the valence band of O^{2–} to the conductivity band^{25–30} should be observed in a region of 3–4.7 eV (257–413 nm). Formation of free charge carriers should be expected for excitation with the light with $\lambda = 310 \text{ nm}$. It is commonly accepted that the recombination of electron–holes pairs, capture of electrons by oxygen-deficient centers of iron, and a low mobility of holes are determining factors for the low conductivity of iron oxides and poor efficiency of iron oxides as photoelectrodes.^{27,31,32}

Electrons captured by particles of a α -Fe₂O₃ colloid during pulse radiolysis exhibit a broad (at least 500–900 nm) absorption spectrum,³² which is resulted from electrons captured by oxygen-deficient centers of Fe³⁺. No evidence of absorption of free electrons in the conductivity band were found in radiolysis experiments.³² In this work, we established the absorption in an interval of λ values of 400–1000 nm. The same kinetics of absorption relaxation in the whole spectral range indicates the predominant relaxation of one type of carriers, which can be electrons captured oxygen-deficient centers of Fe³⁺.³² The relaxation of such carriers can probably be due to the recombination of electron–hole pairs and relaxation to holes with a low absorption cross section. Unlike α -Fe₂O₃, TiO₂ exhibits a broad absorption spectrum of electrons in the conductivity band and, after relaxation, a much narrower absorption band inherent in electrons captured by traps.³² The shift of the absorption band followed by its narrowing is a substantial property of the relaxation of photoinjected "hot" electrons in the conductivity band followed by capturing in traps.^{29,32} The absence of this characteristic feature for the oxide/hydroxides suggests that the thermalization of electrons photoinjected in the

Table 1. Parameters A_1 , A_2 and τ_1 , τ_2 for curves of absorption relaxation determined using the approximation of the experimental curves by the function $A_1\exp(-t/\tau_1) + A_2\exp(-t/\tau_2)$

Sample	$(\tau_1)^{-1} \cdot 10^{-3}$		$(\tau_2)^{-1} \cdot 10^{-4}$		$A_1/(A_1 + A_2)$	$A_2/(A_1 + A_2)$
	fs ⁻¹					
	I ^a	II ^b	I ^a	II ^b		
α -Fe ₂ O ₃	4.7±2.0	2.8	1.2±0.2	0.24	0.66±0.12	0.34±0.12
γ -Fe ₂ O ₃	3.5±1.1	2.8	0.8±0.3	0.24	0.63±0.10	0.37±0.10
α -Fe ₂ O ₃ , Nafion®	6.8±0.7	—	1.7±0.6	—	0.70±0.02	0.30±0.03
Fe ₂ O ₃ , ferritine	4.6±0.8	—	0.7±0.3	—	0.61±0.04	0.39±0.04

^a The results of this work.

^b Published data.¹⁶

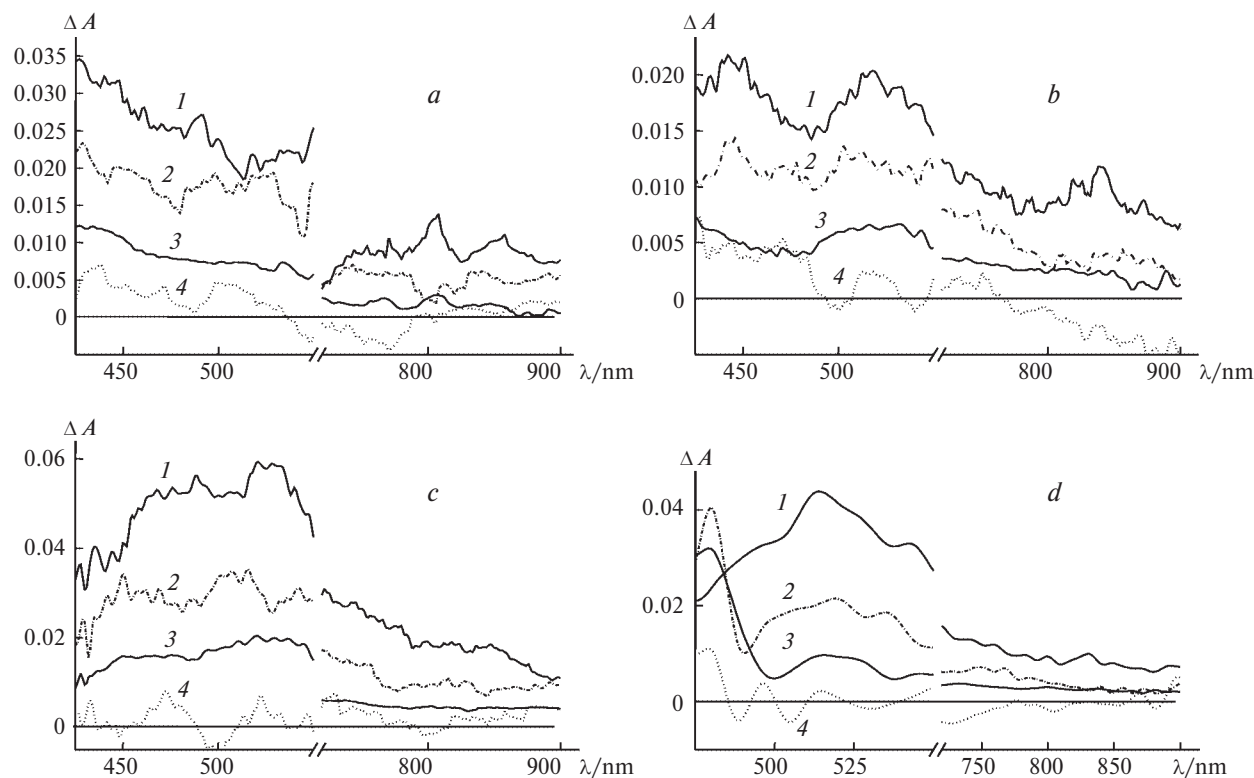


Fig. 3. Transient absorption spectra during the excitation by the femtosecond light pulse with $\lambda = 310$ nm of the samples: α - Fe_2O_3 (a), γ - Fe_2O_3 (b), α - Fe_2O_3 in Nafion® (c), and ferrihydrite $\text{Fe}_2\text{O}_3 \cdot 9\text{H}_2\text{O}$ in the protein shell of ferritine (d). Delay time/fs: 1, 100; 2, 500; 3, 6000; and 4, -150 fs. Time delays are indicated in figures for each spectrum.

conductivity band occurs in the iron oxides within the time shorter than the resolution time (75 fs). This assumption agrees with the results of the work,²⁰ in which the authors estimated this time as being shorter than 150 fs.

The studied nanosized particles of the iron oxides and ferrihydrite differ strongly in crystal structure.³³ The unit cell of the γ - Fe_2O_3 crystal is cubic, and the iron ions are octahedrally and tetrahedrally coordinated (defects of the spinel structure). The unit cell of α - Fe_2O_3 is hexagonal, and all iron atoms are octahedrally coordinated (corundum structure). The α - Fe_2O_3 particles in Nafion®, unlike the colloidal aqueous form of α - Fe_2O_3 , exist in aqueous-ionic water clusters surrounded by the SO_3 groups. The size of these clusters is determined by the internal structure of the Nafion® membrane and close to 4 nm. The iron hydroxide particles bound to the ferritine protein represent one of the main forms in which iron is present in living organisms. Differed in details, ferritines of all types have a resembling molecular architecture: 24 protein subunits form a compact spherical shell ~12 nm in diameter containing a nucleus, which consists of one or several nanosized particles of hydrated iron oxide.^{16,17} The size of the particles is restricted by the size of the internal cavity of ferritine, whose diameter is 8 nm. The crystal structure of the iron particles forming the ferritine

nucleus of mammals is close to that of the natural mineral ferrihydrite $9\text{Fe}_2\text{O}_3 \cdot 5\text{H}_2\text{O}$.³⁴ Ferrihydrite has a hexagonal crystalline lattice in which the iron atoms are octahedrally coordinated and arranged between the layers of the O atoms. However, some iron atoms (to 10%) in the nanosized particles of the iron hydroxide in ferritine are coordinated with five oxygen atoms and one phosphate group. The chemical composition of the nanosized iron hydroxide particles in ferritine is sometimes described as $[\text{FeO}(\text{OH})]_8[\text{FeO}(\text{H}_2\text{PO}_4)]$. The most part of phosphate groups are coordinated to the iron atoms on the crystal surface and serve for binding the iron hydroxide nanocrystals with the protein shell of ferritine.

Thus, we found a great resemblance of the spectra and kinetics of absorption relaxation in all studied forms of iron oxide/hydroxide (α - Fe_2O_3 , colloidal solutions in water and nanosized particles in Nafion®; γ - Fe_2O_3 and nanosized crystal of ferrihydrite $5\text{Fe}_2\text{O}_3 \cdot 9\text{H}_2\text{O}$ in the protein shell). This indicates an important specific feature of the dynamics of relaxation of charge carriers in iron oxides compared to other semiconductors: the absence of a substantial influence of structural differences of the iron oxides and distinctions in properties of the surface and surface environment on the nature of electronic states responsible for the dynamics of photogenerated charge carriers.

This work was financially supported by the Russian Foundation for Basic Research (Project Nos. 00-03-32254, 99-04-49428, and 00-03-40118) and the International Association for Assistance of Cooperation with Scientists of the Former Soviet Union (INTAS) (Grant 554).

References

1. R. M. Cornell and U. Schwermann, *The Iron Oxides*, VCH, Weinheim—New York, 1996.
2. J. Bandara, J. A. Mielczarski, and J. Kiwi, *Langmuir*, 1999, **15**, 7680.
3. C. Guillard, C. Hoangvan, P. Pichat, and F. Marme, *J. Photochem. Photobiol. A: Chem.*, 1995, **89**, 221.
4. K. Hustert and P. N. Moza, *Fresenius Environ. Bull.*, 1994, **3**, 762.
5. C. Kormann, D. W. Bahnemann, and M. R. Hoffmann, *J. Photochem. Photobiol. A: Chem.*, 1989, **48**, 161.
6. H. Miyoshi, H. Mori, and H. Yoneyama, *Langmuir*, 1991, **7**, 503.
7. C. Pulgarin and J. Kiwi, *Langmuir*, 1995, **11**, 519.
8. A. B. Rives, T. S. Kulkarni, and A. L. Schwaner, *Langmuir*, 1993, **9**, 192.
9. C. Siffert and B. Sulzberger, *Langmuir*, 1991, **7**, 1627.
10. H. Yoneyama, *Research on Chem. Intermediates*, 1991, **15**, 101.
11. R. S. Underhill and G. J. Liu, *Chem. of Mater.*, 2000, **12**, 2082.
12. Q. Wang, Q. Sun, M. Sakurai, J. Z. Yu, B. L. Gu, K. Sumiyama, and Y. Kawazoe, *Phys. Rev. B*, 1999, **59**, 12672.
13. J. K. Leland and A. J. Bard, *J. Phys. Chem.*, 1987, **91**, 5076.
14. D. Mauzerall, *Photosynth. Research*, 1992, **33**, 163.
15. R. C. Barry, J. L. Schnoor, B. Sulzberger, L. Sigg, and W. Stumm, *Water Research*, 1994, **28**, 323.
16. S. C. Andrews, *Adv. Microbiol. Physiol.*, 1998, **40**, 281.
17. D. N. Chasteen and P. M. Harrison, *J. Struct. Biol.*, 1999, **126**, 182.
18. M. Aubailly, R. Santus, and S. Salmon, *Photochem. Photobiol.*, 1991, **54**, 769.
19. V. V. Nikandrov, C. K. Gratzel, J. E. Moser, and M. Gratzel, *J. Photochem. Photobiol. B: Biol.*, 1997, **41**, 83.
20. N. J. Cherepy, D. B. Liston, J. A. Lovejoy, H. M. Deng, and J. Z. Zhang, *J. Phys. Chem. B*, 1998, **102**, 770.
21. M. I. Litter and M. A. Blesa, *Canad. J. Chem.*, 1992, **70**, 2502.
22. B. C. Faust, M. N. Hoffman, and D. W. Bahnemann, *J. Phys. Chem.*, 1989, **93**, 6371.
23. F. E. Gostev, A. A. Kachanov, S. A. Kovalenko, O. M. Sarkisov, and A. G. Titov, *Instrum. Exper. Techn.*, 1996, **39**, 567.
24. S. A. Kovalenko, A. L. Dobryakov, J. Ruthmann, and N. P. Ernsting, *Phys. Rev.*, 1999, **A59**, 2369.
25. D. M. Sherman and T. D. Waite, *Am. Mineral.*, 1985, **70**, 1262.
26. M. P. Dare-Edwards, J. B. Goodenough, A. Hamnett, and P. R. Trevelick, *J. Chem. Soc., Faraday Trans. 1*, 1983, **79**, 2027.
27. Z. Zhang, C. Boxall, and G. H. Kelsall, *Colloid Surf. A*, 1993, **73**, 145.
28. N. J. Cherepy, D. B. Liston, J. A. Lovejoy, H. Deng, and J. Z. Zhang, *J. Phys. Chem. B*, 1988, **102**, 770.
29. J. Z. Zhang, *J. Phys. Chem. B*, 2000, **104**, 7239.
30. M. Anderman and J. H. Kennedy, in *Semiconductor Electrodes*, Ed. H. O. Finklea, Elsevier, New York, 1988, 147.
31. C. Leygraf, M. Hendewerk, and G. Somorjai, *J. Solid State Chem.*, 1983, **48**, 357.
32. N. M. Dimitrijevic, D. Savic, O. I. Micic, and A. J. Nozik, *J. Phys. Chem.*, 1984, **88**, 4278.
33. H. Massover, *Micron*, 1993, **24**, 389.
34. S. Mann, J. M. Williams, A. Treffry, and P. M. Harrison, *J. Mol. Biol.*, 1987, **198**, 405.

Received July 2, 2001;
in revised form December 17, 2001